STRUCTURAL ASSESSMENT OF TUNGSTEN-EPOXY BONDING IN SPACECRAFT COMPOSITE ENCLOSURES WITH ENHANCED RADIATION PROTECTION

M. Kanerva[1], J.R. Koerselman[1], H. Revitzer[2], L-S. Johansson[3], E. Sarlin[4], A. Rautiainen[5], T. Brander[1], and O. Saarela[1]

[1]*Aalto University, School of Engineering, Department of Applied Mechanics, P.O.Box 14300, FI-00076 Aalto, email: Mikko.Kanerva@aalto.fi*

[2]*Aalto University, School of Chemical Technology, Department of Chemistry, P.O.Box 14300, FI-00076 Aalto*

[3]*Aalto University, School of Chemical Technology, Department of Forest Products Technology, P.O.Box 14300, FI-00076 Aalto*

[4]*Tampere University of Technology, Department of Material Science, P.O.Box 589, FI-33101 Tampere*

[5]*Aalto University, School of Electrical Engineering, Department of Electrical Engineering and Automation, P.O.Box 14300, FI-00076 Aalto*

ABSTRACT

Spacecraft include sensitive electronics that must be protected against radiation from the space environment. Hybrid laminates consisting of tungsten layers and carbon-fibre-reinforced epoxy composite are a potential solution for lightweight, efficient, and protective enclosure material. Here, we analysed six different surface treatments for tungsten foils in terms of the resulting surface tension components, composition, and bonding strength with epoxy. A hydrofluoric-nitric-sulfuric-acid method and a diamond-like carbon-based DIARC® coating were found the most potential surface treatments for tungsten foils in this study.

Key words: Tungsten surface treatment; Hybrid laminate; Radiation protection.

1. INTRODUCTION

Various electronic systems as well as instruments for scientific measurements are placed inside protective enclosures in spacecraft. An enclosure must possess sufficient structural rigidity and it must introduce radiation protection in order to form a shield against electrons, protons and small particles from the surrounding space environment. Metallic materials, such as aluminium alloys, are relatively stiff and the atomic weight is a proper compromise to shield systems from both electrons and protons. However, the requirement for ever lower weight in spacecraft structures tempts to use composite and hybrid materials in the enclosures [3, 4]. In particular, the radiation protection features of an enclosure can be optimised without compromises by using stainless steel or tungsten layers combined with carbon-fibre-reinforced epoxies (CFRP) [6, 8].

In this work, we analyse six different surface treatments for thin tungsten foils to manufacture a hybrid laminate using CFRP pre-pregs. In general, the adhesion between the tungsten foils and CFRP of the cured hybrid laminate should be as high as possible. Likewise, the surface quality of the treated tungsten foils should be constant over a large area. Moreover, the laminate structure should be well-defined so that it could be reliably modelled for the radiation protection optimization. Here, we focus on chemical treatments and coatings for tungsten foils and not on mechanical roughening.

2. EXPERIMENTAL

2.1. Raw material and laminate preparation

Tungsten foils with a nominal thickness of 50 µm and 99.95% purity were provided by Alfa Aesar GmbH (Germany). Unidirectional CFRP pre-preg tape was acquired from Advanced Composites Group (ACG, Umeco, UK), with a nominal thickness of 0.29 mm, 300 g/sqm areal weight and 32% (w/w) resin content. The pre-preg consisted of M40J(12K) high modulus carbon fibres (Toray, USA) impregnated with an MTM® 57 epoxy resin (ACG, UK). Laminates for mechanical testing were cured according to the instructions of the pre-preg manufacturer using an autoclave (60 min hold at 120 °C) and vacuum bagging (0.95 bar vacuum). For bonding studs to tungsten foils for pull-off testing, a room temperature curing DP190 epoxy paste adhesive (3M, USA) was used.

2.2. Tungsten surface treatments

Six different surface conditions of tungsten were studied, as shown in Table 1. The effect of tungsten oxidation

Table 1. The studied surface treatments for tungsten foils

Series	Treatment	Ref.
Oxidation	Six-stage cleaning process and oxidation at 400 °C for 60 min.	[7]
Caustic soda	Immersion in a mixture of sodium hydroxide and MilliQ water at room temperature, followed by rinsing in MilliQ water and drying in air flow (82–84 °C).	[2]
HFNS acid	Immersion in a mixture of hydrofluoric acid (60%) 5 pbw, nitric acid 30 pbw, sulfuric acid 50 pbw and MilliQ water 15 pbw (+ few drops of hydrogen peroxide) at room temperature, followed by rinsing in MilliQ water and drying in an oven (70 °C, 15 min).	[5]
Sol-gel	Application of AC-130-2 sol-gel by brush, followed by 10 minutes of drying at room temperature.	[1]
Diarc	0.1 µm thick DIARC® coating by Diarc-Technology Oy.	-
Cu-Ni-Au	3 µm thick copper-nickel-gold gradient coating by Eforit Oy.	-

on adhesion was studied by oxidizing tungsten foils at 400 °C for 60 minutes; prior to the oxidation, the foils were cleaned using a cleaning procedure as described in [7]. Chemical surface treatments included a caustic soda method, a hydrofluoric-nitric-sulfuric-acid (HFNS) method and a sol-gel method. Also, two coating methods were studied: a diamond-like carbon-based coating DIARC® (Diarc-Technology Oy, Finland) and a gradient copper-nickel-gold (Cu-Ni-Au) coating by a tailored electrolytic-electroless deposition (Eforit Oy, Finland). Prior to a chemical treatment or a coating process, the foils were degreased using methyl ethyl ketone (MEK).

2.3. Pull-off testing

Different tungsten surface treatments were screened using pull-off testing as described in the standard ASTM D 4541. Each pull-off test was conducted on a 4 cm × 4 cm tungsten foil. Prior to testing and specimen bonding procedures, a bulky CFRP plate and standard aluminium studs were grit blasted, and the studs were also treated using the cleaning procedure [7] with optimised immersion time (three minutes). The treated studs were bonded on the tungsten pieces using DP190 adhesive and also scrim cloth for controlling the adhesive thickness. Second, the stud-tungsten specimens were bonded to the CFRP plate, as shown schematically in Fig. 1. The bonded specimens were cured at room temperature for 42 hours and post-cured for six hours at 50 °C. The bonded specimens were tested using the Elcometer 110 Patti pneumatic adhesion tester (Elcometer, UK). The pull-off strength, σ_u, was calculated as follows:

$$\sigma_u = \frac{p_f \cdot C_N}{A_{st}}, \quad (1)$$

where p_f is the applied pressure at the time of bond failure, C_N is a factor provided by the instrument manufacturer for converting applied pressure to pull-off force in Newtons, and A_{st} is the stud's bond area.

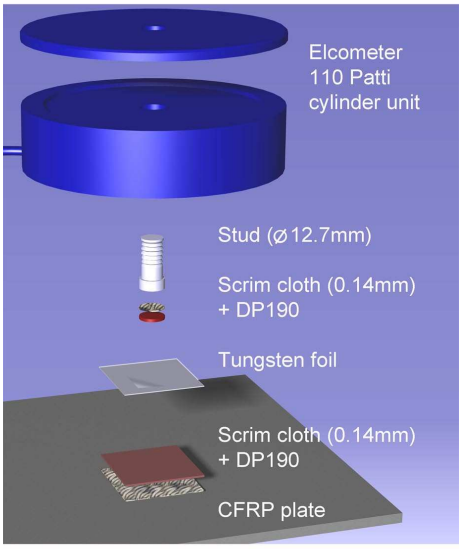

Figure 1. The test setup and specimen bonding scheme for pull-off testing (ASTM D 4541).

2.4. Contact angle measurements

The effect of immersion time on the wetting and surface tension for the HFNS method was studied using contact angle measurements. Sessile drop measurements were conducted using the CAM 200 system (KSV Instruments, Finland). Three different probe liquids, as shown in Table 2, were applied with a nominal drop size of 2.5 µl. For each tungsten foil sample, five different drops per probe liquid were measured on different locations on a sample surface to account for spatial variation in the surface quality, and three measurements on each drop with one-second time interval were performed to account for operator-dependent errors. Finally, mean contact angles were calculated for the probe liquids. Three series of tungsten foils were prepared so that they were first gently roughened using Scotch-Brite™ and then surface treated using the HFNS method with different immersion time in the acid mixture (60, 180, 300 seconds) in addition to a control surface with only a degrease using MEK.

We started our surface tension analysis by recalling the Young's equation:

$$\sigma_{SL} = \sigma_{SV} - \sigma_{LV}\cos\theta \quad (2)$$

where σ_{SL} is the (interfacial) surface tension at the substrate–liquid interface, σ_{SV} is the (interfacial) surface tension at the substrate–vapour interface, σ_{LV} is the (interfacial) surface tension at the liquid–vapour interface, and θ is the contact angle. At any interface, surface tension can be thought to include dispersive (superscript d) and polar (superscript p) forces, so that $\sigma_{ij} = \sigma_{ij}^d + \sigma_{ij}^p$. Further splitting requires considering the free energy of adhesion and applying the Dupré equation for either of the components:

$$\Delta G_{ij}^{d/p} = \gamma_{ij}^{d/p} - \gamma_i^{d/p} - \gamma_j^{d/p}\,, \quad (3)$$

where γ refers to specific surface energy and ΔG refers to the free energy of adhesion at an interface between substances i and j. The challenge in Eq. 3 is that the γ_{ij} terms cannot be directly determined by measurements. For solving the problem, so-called Lewis acid-base interaction parameters are applied [11]:

$$\Delta G_{ij}^{p} \equiv -2\sqrt{\gamma_i^{\ominus}\gamma_j^{\oplus}} - 2\sqrt{\gamma_j^{\ominus}\gamma_i^{\oplus}}\,, \quad (4)$$

where superscripts $\oplus$ and $\ominus$ refer to electron accepting and electron donating interaction, respectively. Substitution of Eq. 4 into Eq. 3 gives:

$$\gamma_{ij}^{p} = 2\left(\sqrt{\gamma_i^{\ominus}\gamma_i^{\oplus}} + \sqrt{\gamma_j^{\ominus}\gamma_j^{\oplus}} - \sqrt{\gamma_i^{\ominus}\gamma_j^{\oplus}} - \sqrt{\gamma_j^{\ominus}\gamma_i^{\oplus}}\right)$$

$$\Rightarrow \quad \gamma_{ij}^{p} = \gamma_i^{p} + \gamma_j^{p} - 2\left(\sqrt{\gamma_i^{\ominus}\gamma_j^{\oplus}} + \sqrt{\gamma_j^{\ominus}\gamma_i^{\oplus}}\right). \quad (5)$$

The dispersive Lifshitz-van der Waals interactions in turn have been defined using the combining rule [12]:

$$\gamma_{ij}^{d} \equiv \gamma_i^{d} + \gamma_j^{d} - 2\sqrt{\gamma_i^{d}\gamma_j^{d}}\,. \quad (6)$$

By presuming that there is insignificant interaction between substrate and vapour as well as between liquid and vapour, we can rewrite the Young's equation:

$$\sigma_{SL} = \sigma_S - \sigma_L cos\theta\,. \quad (7)$$

By estimating $\gamma_{SL}^d + \gamma_{SL}^p \approx \sigma_{SL}^d + \sigma_{SL}^p = \sigma_{SL}$ and by substituting Eqs. 5 and 6 into Eq. 7 we arrive to:

$$\sigma_L(1+\cos\theta) = 2\left(\sqrt{\sigma_S^d\sigma_L^d} + \sqrt{\sigma_S^{\ominus}\sigma_L^{\oplus}} + \sqrt{\sigma_L^{\ominus}\sigma_S^{\oplus}}\right), \quad (8)$$

which is also known as the van Oss-Chaudhury-Good (OCG) equation. Eq. 8 involves three unknown parameters (σ_S^d, $\sigma_S^{\ominus}$, $\sigma_S^{\oplus}$), which can be solved from the contact angle measurements using three probe liquids (at a minimum). A coarse, first estimate of the parameters σ_S^d and σ_S^p can be determined using a simplified version of the OCG equation [10]:

$$\sigma_L(1+\cos\theta) = 2\left(\sqrt{\sigma_S^d\sigma_L^d} + \sqrt{\sigma_S^p\sigma_L^p}\right). \quad (9)$$

Eq. 9 can be transformed into a linear form $V = mH + b$ using the following notations [9]:

$$H = \sqrt{\frac{\sigma_L - \sigma_L^d}{\sigma_L^d}} = \sqrt{\frac{\sigma_L^p}{\sigma_L^d}}\,, \quad m = \sqrt{\sigma_S^p}\,,$$

$$V = \frac{1+\cos\theta}{2}\cdot\frac{\sigma_L}{\sqrt{\sigma_L^d}}\,, \quad b = \sqrt{\sigma_S^d}\,,$$

so that the values of σ_S^d and σ_S^p can be solved by presenting the contact angle measurement data in a H–V plot and least-squares-fitting a line.

Table 2. Probe liquids used for the contact angle measurements

Liquid	σ_L (N/m)	σ_L^d (N/m)	σ_L^p (N/m)
Deionized water	0.0728	0.0218	0.051000
Glycerol	0.0640	0.0340	0.030001
Ethylene glycol	0.0480	0.0290	0.018999

2.5. Field-emission scanning electron microscopy (FESEM) and X-ray energy dispersive spectroscopy (EDS)

Fracture surfaces were studied using the field-emission scanning electron microscope ULTRAplus (Zeiss, Germany). Samples were extracted from larger specimens or mounted and polished by typical procedures for preparing a cross-sectional sample. In addition, elemental composition of the samples was studied using INCAx-act (Oxford Instruments, UK) X-ray energy dispersive analyser, which was installed to the FESEM microscope.

2.6. X-ray photoelectron spectroscopy (XPS)

X-ray photoelectron spectroscopy was utilised in surface analysis of the HFNS-treated tungsten foils, using the AXIS Ultra electron spectrometer (Kratos Analytical, UK) and CasaXPS software. Data was recorded using monochromatic Al Kα X-rays at 100 W. Surveys were recorded at 160 eV pass energy and 1 eV step and the high resolution regions at 20 eV pass energy and 0.1 eV step. Fresh cellulose sample was used as an *in-situ* reference with each measurement batch.

2.7. Single-lap shear testing and tensile testing

The effect of immersion time on the bond strength of tungsten-CFRP hybrids with the HFNS method was stud-

ied using single-lap shear testing described in the standard ASTM D 5868. Prior to the lamination of the specimens, three series of tungsten (W) foils were gently roughened using Scotch-Brite™ roughening sponges and treated using the HFNS method with different immersion times in the acid mixture (60, 180, 300 seconds). A $(0/\pm45/90/0)_{so}$ lay-up was applied for the specimen arms and aluminium shimming plates were used in preparing the overlapping. The overall mechanical performance of a tungsten-CFRP hybrid laminate, with a $(0/\pm45/90/W)_{so}$ lay-up, was studied using tensile testing described in the standard ASTM D 3039. A computerized (MTS, USA) universal testing machine was used and loading rates of 13 mm/min and 2 mm/min were applied during the lap-shear tests and tensile tests, respectively. A schematic illustration of the test specimens' dimensions and lay-ups is shown in Fig. 2.

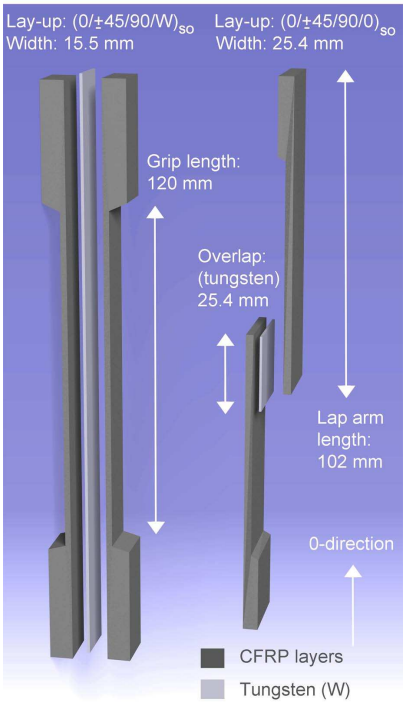

Figure 2. CFRP–tungsten specimen configurations and nominal dimensions for tensile testing (ASTM D 3039) and single-lap shear testing (ASTM D 5868).

3. RESULTS AND ANALYSIS

3.1. Tungsten-epoxy bonding strength

The determined pull-off strength values and observed failure loci for different tungsten-epoxy bonds are shown in Table 3. The oxidation treatment and caustic soda method resulted in the lowest pull-off strength values and also led to more than 50% adhesive failure. The sol-gel method was seen as a potential treatment, although there was a great scatter in the strength values and failure loci between the three tested specimens. The sol-gel was at the end of its shelf life and this might have affected the resulting surface quality. On the contrary, the HFNS method as well as the DIARC and Cu-Ni-Au coatings increased the pull-off strength significantly.

The Cu-Ni-Au coating fractured near the tungsten-coating interface and a more detailed analysis was conducted using FESEM and EDS. First, local EDS results, shown in Fig. 3, indicated that the stud's side fracture surface contained essentially Ni and that no observable traces of W, Cu or Au were detected. Second, cross-sectional EDS mapping, shown in Fig. 4, confirmed that the fracture occurred either at the Ni-Au interface or Au-W interface, and that the Cu-rich region was intact

Table 3. Determined pull-off strength values (mean ± standard deviation) and related failure loci for different tungsten-epoxy bonds

Series	Studs tested	Pull-off strength (MPa)	Mean adhesive failure area (%)
Oxidation	4	6.8±1.6	≈98
Caustic soda	4	6.6±1.3	≈58
HFNS (60 sec)	4	9.2±1.1	≈51
Sol-gel	3	7.1±2.9	≈40
Diarc	4	14.0±2.4	≈50
Cu-Ni-Au	4	10.7±5.0	≈95

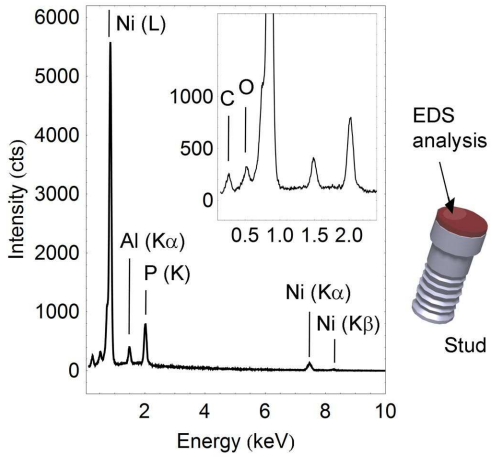

Figure 3. EDS spectrum of an analysis conducted on the fracture surface of a Cu-Ni-Au specimen after pull-off testing (the stud's side fracture surface).

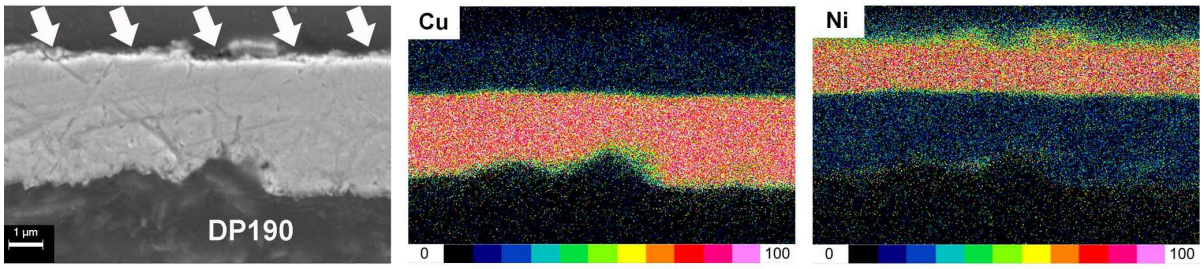

Figure 4. Cross-sectional FESEM image and EDS maps on a fractured Cu-Ni-Au specimen after pull-off testing (sample cut from the stud's side). The white arrows show the fracture path in the cross-section.

3.2. The effect of acid immersion time for the HFNS surface treatment method

The HFNS surface treatment method was further studied since it was seen that there was a potential for optimizing the immersion time in acid mixture. The results of the contact angle measurements for the tungsten foils with different immersion times are shown in Table 4. It can be seen that the wetting of the tungsten surface was enhanced in the case of each probe liquid, when the HFNS method was applied. However, there was a very little effect by the immersion time especially when considering the standard deviations per series and per each probe liquid. The first estimates of the tungsten surface tension components, shown in Table 5, also suggest a very little effect by the immersion time but a marked increase in the total surface tension ($\Delta\sigma_S \approx 53\%$) due to the HFNS method in general.

Table 4. Measured sessile drop contact angles (mean ± standard deviation) for tungsten surfaces, which were treated using the HFNS method and different immersion times

Immersion time (sec)	Contact angle with water (°)	Contact angle with glycerol (°)	Contact angle with ethylene glycol (°)
0 (control)	61.47±5.3	66.93±1.3	50.85±2.3
60	33.70±4.0	38.17±4.2	19.77±3.4
180	33.57±4.5	36.78±3.8	23.61±3.7
300	33.89±3.9	35.93±6.3	19.99±2.7

A more detailed analysis of the surface tension components was conducted by adapting the exact OCG equation. The three unknown components (σ_S^d, $\sigma_S^{\ominus}$, $\sigma_S^{\oplus}$) for each tungsten surface were determined iteratively using a constrained minimisation algorithm of a Wolfram Mathematica 9.0 software (Wolfram Research Inc., UK). The determined components are shown in Table 6. In general, the total surface tension of the treated foils was slightly higher when using the exact OCG equation. This deviation was mostly due to the precise term for the acid-base interaction; the polarity (σ_S^p) using the exact OCG equation was higher for the treated tungsten surfaces but lower for the control series when compared to the results using the simplified OCG. The difference between the immersion times was not marked; all the tungsten foil samples, which had been treated using the HFNS method, were highly polar. This effect was also observable in the results by the simplified OCG equation. The average increase in the total surface tension due to the HFNS method, determined using the exact OCG equation, was ≈150%.

Table 5. First estimates of surface energy components of tungsten foils, which were treated using the HFNS method and different immersion times

Immersion time (sec)	σ_S (N/m)	σ_S^d (N/m)	σ_S^p (N/m)
0 (control)	0.0453	0.0029	0.0425
60	0.0694	0.0044	0.0650
180	0.0693	0.0044	0.0649
300	0.0700	0.0044	0.0655

Table 6. Determined dispersive Lifshitz-van der Waals interaction parameters and the Lewis acid-base interaction parameter for tungsten foils, which were treated using the HFNS method and different immersion times

Immersion time (sec)	σ_S^d (N/m)	σ_S^p (N/m)	$\sigma_S^{\oplus}$ (N/m)	$\sigma_S^{\ominus}$ (N/m)
0 (control)	0.0095	0.0232	0.0038	0.0354
60	7.8E-5	0.0847	0.0300	0.0610
180	0.0009	0.0741	0.0242	0.0567
300	2.8E-5	0.0850	0.0301	0.0600

3.3. The effect of HFNS surface treatment method on CFRP-tungsten hybrid laminates

The bonding strength for tungsten-CFRP laminates was studied using single-lap shear testing. The determined shear strength values (mean ± standard deviation based on five specimen per series) were 16.9 ± 1.7 MPa, 16.7 ± 1.2 MPa and 11.9 ± 0.6 MPa, for an immersion time of 60, 180 and 300 seconds, respectively. These values give an indication that an immersion time longer than 180 seconds would result in a decrease in the interface strength and that already a 60-second immersion is long enough for good adhesion. The determined tensile values (mean ± standard deviation of four specimens) for a tungsten-CFRP hybrid laminate (HFNS method with a 60-second immersion) were as follows: Young's modulus was 67 ± 3 GPa, first failure stress 266 ± 34 MPa and ultimate stress 696 ± 13 MPa. The first failure was due to extensive delamination of the tungsten foil, and this was assumed to be the result of high residual stresses inside the laminate, due to thermal expansion mismatch. The internal structure of the rolled tungsten foils was also found weak. More details about the mechanical testing of the tungsten-CFRP hybrid laminates can be found in [8].

3.4. Tungsten surface oxide layer composition

The effect of the HFNS method on the composition of the oxide layer on tungsten surface was studied using XPS. A control sample, which was only degreased using MEK, was analysed first. For making a comparison, a tungsten foil, which was degreased using MEK and subsequently treated using the HFNS method with a 67-second immersion time, was analysed. At a minimum, six spectra per sample were collected. The results are shown in Table 7. It can be seen that the amount of oxygen has reduced due to the HFNS treatment—presumably due to etching (dissolution) of the original oxide layer. The increases in carbon, nitrogen and sulphur content for the HFNS-treated tungsten foil were presumed contamination from the acid mixture. Faint traces (At. % < 0.6) of sodium were observed, too.

Table 7. Tungsten surface atomic concentrations (mean ± standard deviation) based on the XPS spectra

Tungsten surface	C1s (At. %)	O1s (At. %)	W4d (At. %)	N1s (At. %)	S2p (At. %)
MEK-cleaned	27.7 ±1.6	49.4 ±1.1	17.2 ±0.7	5.0 ±0.5	0.1 ±0.1
HFNS-treated	31.8 ±6.9	40.8 ±5.7	15.6 ±2.3	7.9 ±1.3	3.8 ±0.8

4. CONCLUSIONS

Tungsten-CFRP systems were studied to develop structurally feasible, radiation protective laminate material for spacecraft enclosures. A hydrofluoric-nitric-sulfuric-acid (HFNS) method and a diamond-like carbon-based coating DIARC® were found efficient surface treatments for adhesively bonding tungsten and epoxy. It was found that the HFNS method increases the tungsten surface polarity approximately 250 percent, total surface tension approximately 150 percent and also affects the oxide layer composition in terms of decreased oxygen content. Future studies are needed to optimise the effects of the HFNS surface treatment on tungsten foils and also to analyse the internal residual stresses in tungsten-CFRP hybrid laminates.

ACKNOWLEDGEMENTS

Dr J.M. Campbell is greatly acknowledged for performing the XPS measurements.

The research leading to these results has received funding from the European Community's Seventh Framework Programme (FP 7 / 2007-2013) under Grant Agreement n° 262746.

REFERENCES

[1] 2008, AC-130® metal alloy surface preparation for bonding, Tech. rep., AC-Tech, USA

[2] 2014, Surface preparation and pretreatment for structural adhesives, Tech. rep., 3M, USA

[3] Aglietti, G. 2002, J Aerospace Eng, 216, 131

[4] Gaier, J., Hardebeck, W., Bunch, J., Davidson, M., & Beery, D. 1998, J Mater Res, 13, 2297

[5] Guttmann, W. 1961, Concise guide to structural adhesives (Reinhold), 22–23

[6] Jussila, J. & Brander, T. 2005, in European Conference on Spacecraft Structures, Materials and Mechanical Testing (Proceedings), Noordwijk, The Netherlands, ESA SP-581

[7] Kanerva, M., Sarlin, E., Campbell, J., Aura, K., & Saarela, O. 2013, Eng Fract Mech, 97, 244

[8] Koerselman, R. 2012, Master's thesis, Delft University of Technology, ISBN 978-952-60-4775-1

[9] Lugscheider, E., Bobzin, K., & Möller, M. 1999, Thin Solid Films, 355-356, 367

[10] Owens, D. & Wendt, R. 1969, J Appl Polym Sci, 13, 1741

[11] van Oss, C. 1987, Adv Colloid Interface Sci, 28, 35

[12] van Oss, C. 1988, Chem Rev, 88, 927